





## DESIGNING AN EVOLUTIONARY OPTIMAL WASHOUT FILTER BASED ON GENETIC ALGORITHM

Alireza GHARIB , Masoud GOHARIMANESH ,  
Ali KOOCHI , Mohammad Reza GHARIB \*

*Department of Mechanical Engineering, University of Torbat Heydarieh, Torbat Heydarieh, Iran*

Received 26 November 2020; accepted 15 June 2021

**Abstract.** This paper aims to design a reliable filter that can transform the actual motion of a flight simulator maneuver into a logical and understandable movement for its workspace. Motion cueing algorithms are used in scaling maneuvers to improve the user's perception of real-world motion. As a unique algorithm, the washout-filter algorithm reduces the real motions where the user cannot understand the difference between the actual and simulated maneuvers. To design a proper washout filter, first, apply the inner ear model where humans can feel the motion to design a proper filter. The Otolith and semicircular systems were represented by two parts in this model. Second, an evolutionary theory based on a genetic algorithm is used to design a structure that minimizes human perception error and workspace boundaries. The issue is determining the coefficients in the model in order to create a high-performance flight simulator. The filtering algorithm, based upon the human vestibular model, compares human perception with flight simulator motion knowledge. The findings demonstrate an objective function that minimizes user perception error, and the flight simulator motion range can prepare a reliable washout filter for motion cueing.

**Keywords:** washout filter, optimal theory, genetic algorithm, modeling, control, flight simulator.

### Introduction

Washout filter (WF) is the motion algorithm that transforms the movement from actual acceleration to the flight simulator (Grant & Reid, 1997; Parrish et al., 1975; Sivan et al., 1982). This filter's primary intention is to provide motion cues that provide human perception (Song et al., 2002). Moreover, the motion produced must proceed within the limitations, constraints, and bounds of the proposed flight simulator (Wang & Fu, 2004). This filter's most important use is in flight simulators based on the Stewart parallel robot mechanism (Affan et al., 2019).

Many researchers have recently worked on the classical washout filter (CWF), including the high pass and low pass filters (Wang et al., 2008). Although CWFs are famous for their simplicity and adjustability (Liao et al., 2004), they are not reliable due to the decreasing human perception. Recently, the new theories for applying WF have been grown up. The optimal (Asadi et al., 2016; Chen & Fu, 2011; Gharib, 2020; Huang & Fu, 2006; Kong et al., 2016; Sivan et al., 1982), adaptive (Arioui et al., 2005; Chen & Fu, 2010; Huang & Fu, 2006; Parrish et al.,

1975; Wang et al., 2010; Yang et al., 2010) and robust (Asadi et al., 2016; Moavenian et al., 2011; Huang & Fu, 2006; Kim et al., 2006; Salehi Kolahi et al., 2021; Salehi Kolahi et al., 2021; Gharib et al., 2021) theories are the most important ones in this field. An adaptive washout filter (AWF) was introduced by (Nahon et al., 1992) based on the CWF using a self-turning algorithm. An optimal washout filter (OWF) is based on optimal theories (Telban et al., 2002). They solved the Algebraic Riccati Equation (ARE) to provide the proposed requirements. Three kinds of washout filters are based on CWF, AWF, and OWF compared by (Nehaoua et al., 2008). They investigated to see the different performances of these filters in driving flight simulators. Consequently, they have done several methods to present the proficiency of the platform workspace. Asadi et al. (2016) suggested an OWF connected to a genetic algorithm (GA). They designed a compensator after the main OWF and optimized their parameters using GA. The optimization methods were used in different types of WF. Tuning the weight of a predictive washout filter (PWF) was considered (Mohammadi et al., 2018b). In other research (Mohammadi et al.,

\*Corresponding author. E-mail: [m.gharib@torbath.ac.ir](mailto:m.gharib@torbath.ac.ir)

2018a) used a GA to get the best horizon of an adaptive control system for an AWF. Due to some problems in optimizing the classical filter parameters, the adaptive filter approach has been considered recently. Qazani et al. (2020) employed this type of filter for a flight simulator placed on a parallel robot platform with six degrees of freedom. The complexity of the relationships in optimal, adaptive, and resistant filters is so great that it makes it difficult to apply these filters in reality. Liu et al. (2020) considered the application of a classical filter in reality. This is why it can be seen in practical projects that the classic filter is still very popular and accepted. However, having a set of rules in the formation of the classic filter can be very effective and useful. For this reason, some studies like (Asadi et al., 2019) use fuzzy logic as a facilitator.

In this study, we also use a classical filter, and with fundamental changes on the required transfer functions, we find the best case using evolutionary algorithms. Then, by inspiring OWE, an evolutionary optimal washout filter (EOWF) based on a genetic algorithm is designed. The goal is to minimize the perception error and proceed with the flight simulator’s workspace’s actual action. The rest of the paper is organized as follows. Firstly, the OWF and human perception systems are described thoroughly. By inspiring OWE, the new EOWF is introduced, and finally, the result of the simulation is discussed.

### 1. Optimal washout filter design

The optimal control technique applied to the algorithm washout filter is shown in Figure 1. This algorithm’s objective function includes the perception error and the constraints related to the workspace motion. Where  $a_A$  and  $a_s$  are the acceleration sensed in the actual and workspace position. Also,  $\omega_A$  and  $\omega_s$  are the rotational velocities sensed in these positions. Due to the use of a dual-input and dual-output model, we need four transform functions ( $W_{11}$ ,  $W_{12}$ ,  $W_{21}$ , and  $W_{22}$ ), each of which can represent each input’s effect on each output.

To consider WF’s structure and parameters, converting the actual input and flight simulator input is necessary. Two different paths to compare the perception of actual motion and simulator are displayed in Figure 2.

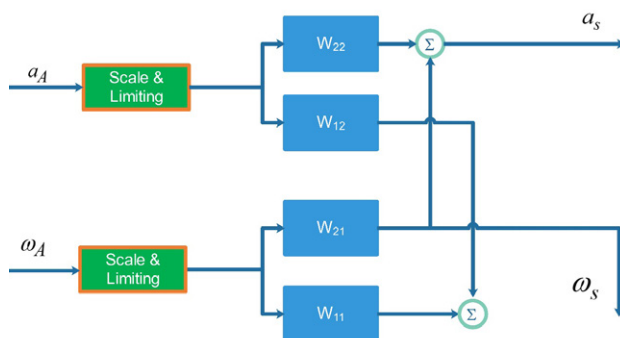


Figure 1. Algorithm of optimal washout filter (OWF) (source: Chen & Fu, 2011)

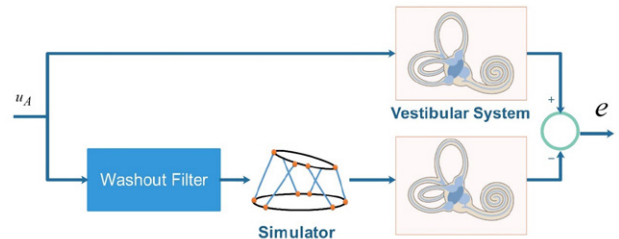


Figure 2. The comparison of the perception in actual and simulator motion

In Figure 2, the upper signal demonstrates the actual motion transmitted by the human vestibular system. The bottom layer shows how actual motion input is filtered by washout algorithm and proceeds with the simulator’s effort. Then, the output of the simulator is sensed by the vestibular model to evaluate human perception. In the ideal condition,  $e$  could be approximated to zero. The differences between the paths are defined as human perception errors in designing the OWF applied.

### 2. Vestibular system modeling

A vestibular system includes two degrees of freedom, surge, and pitch is shown in Figure 3, where  $a_x$ ,  $\dot{\theta}$  are the actual linear acceleration and rotational speed, respectively. Also, the  $\hat{f}_x$  and  $\hat{\theta}$  are the sensed acceleration (specific force) and the rotational speed, respectively. Moreover,  $g$  is the gravity acceleration and  $\int$  defines the integral of the velocity to proceed position.

A simulated model for vestibular systems includes Otolith, semicircular, and the EOWF shown in Figure 4. This model is the extended state of schematics in Figures (1–3).

The tilt coordinate effect on the specific force in the longitudinal model is displayed in Figure 5.

The specific surge force in the central motion of the simulator can be obtained by Eq. (1) (Chen & Fu, 2011):

$$f_x = a_x \cos\theta + g \sin\theta \cong a_x + g\theta. \tag{1}$$

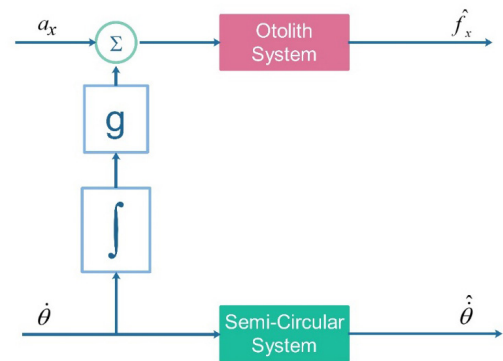


Figure 3. Schematic of a vestibular model includes Otolith and Semicircular systems for human perception facing linear and angular velocity

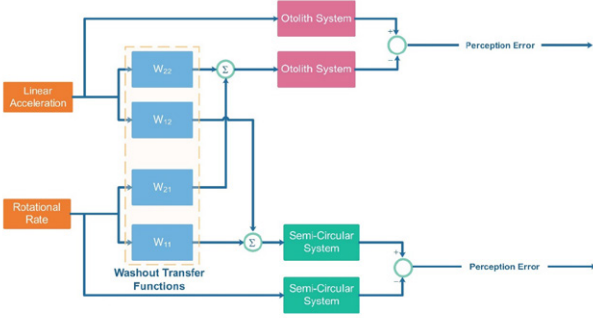


Figure 4. Simulated model of the Otolith and vestibular system in MATLAB/Simulink environment integrated to the washout filter

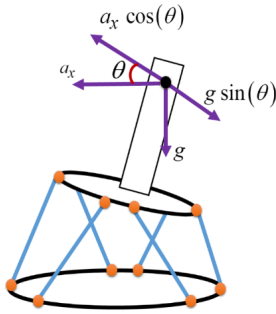


Figure 5. Tilt coordinate effect on the specific force

By regarding the small angles,  $\sin(\theta)$  and  $\cos(\theta)$  could be substituted by  $\theta$  and 1, respectively. The sensed specific force,  $\hat{f}_x$  is related to the stimulus-specific force sensed by the Otolith model is introduced by Eq. (2):

$$\hat{f}_x = \frac{k(\tau_a s + 1)}{(\tau_l s + 1) + (\tau_s s + 1)} f_x, \quad (2)$$

where  $\tau_a$ ,  $\tau_b$ ,  $\tau_s$ , and  $k$  represent the parameters of the Otolith model. By applying Laplace from Eq. (1), a new Laplace form equation can be obtained (3). The term  $(1/s)$  is the integral sign of the angular velocity.

$$f_x(s) = a_x(s) + g \frac{1}{s} \dot{\theta}(s). \quad (3)$$

By substituting Eq. (3) into Eq. (2), we have:

$$\hat{f}_x = \frac{k\tau_a s + k}{\tau_l \tau_s s^2 + (\tau_s + \tau_l)s + 1} \left( a_x(s) + g \frac{1}{s} \dot{\theta}(s) \right). \quad (4)$$

The sensed angular velocity,  $\hat{\theta}$  is related to the actual angular velocity sensed by the semicircular system (Chen & Fu, 2010).

$$\hat{\theta} = \frac{\tau_a \tau_l s^2}{(\tau_l s + 1) + (\tau_s s + 1) + (\tau_a s + 1)} \dot{\theta}. \quad (5)$$

Equation (5) can be rewritten as:

$$\hat{\theta} = \frac{T_3 s^2}{s^3 + T_2 s^2 + T_1 s + T_0} \dot{\theta}, \quad (6)$$

where  $T_0$ ,  $T_1$ ,  $T_2$ , and  $T_3$  are constants and can be defined by:

$$\begin{aligned} T_0 &= 1/(\tau_a \tau_l \tau_s), \\ T_1 &= (\tau_a + \tau_l + \tau_s)/(\tau_a \tau_l \tau_s), \\ T_2 &= (\tau_a \tau_l + \tau_l \tau_s + \tau_a \tau_s)/(\tau_a \tau_l \tau_s), \\ T_3 &= (\tau_a \tau_l)/(\tau_a \tau_l \tau_s). \end{aligned} \quad (7)$$

The actual input signal vector for the rest of the processing is considered as  $u_a(s) = [a_x(s) \quad \dot{\theta}(s)]$ .

### 3. Proposed method

By completing the equations and deriving the new terms, a generalized transfer function is generated, connecting the real motion with the flight simulator motion (Chen & Fu, 2011).

$$u_s(s) = W(s)u_a(s), \quad (8)$$

where  $W$  is the matrix of the optimized transfer function transferring the simulator inputs  $u_s(s)$  to the actual motion inputs  $u_a(s)$ . The transfer function  $W(s)$  is defined as a matrix form (Eq. (9)).

$$W(s) = \begin{bmatrix} W_{11} & W_{12} \\ W_{21} & W_{22} \end{bmatrix}. \quad (9)$$

In the above equation, Euler's angles pass through  $W_{11}$  a filter to create the rotating motion. Two types of acceleration are produced by  $W_{12}$ . The low-pass filter presents this filter. This path operates the same as the Tilt coordinate in the classic washout. To transmit the Euler's angles, the transfer function passes through  $W_{21}$ . The transfer function  $W_{22}$  is presented by the high-pass filter, which behaves to reduce low transmission frequencies.

The form of each  $W_{ij}$  is shown in Eq. (10); overall, twelve parameters are used for filling up the numerator and denominators, respectively. The parameters of the denominator are unique for all  $W_{ij}$ .

$$W_{ij} = \frac{a_5 s^5 + a_4 s^4 + a_3 s^3 + a_2 s^2 + a_1 s + a_0}{b_5 s^5 + b_4 s^4 + b_3 s^3 + b_2 s^2 + b_1 s + b_0}. \quad (10)$$

Although using optimal theory and solving ARE is easy, finding the proper matrix for the numerical solution is not straightforward and maybe failed. For this reason, in this paper, we tried to find the optimal parameters using a GA. The objective function for this problem is shown in Eq. (11).

$$CF = \int_0^t |z_s - z_0| + |P_a(a^\dagger) - P_s(a^\dagger)| dt. \quad (11)$$

The flight simulator heave position and the base heave value are considered 0.3 in this paper (The flight simulator's physical constraint). Moreover,  $P_a$  is a perception function that senses  $a^\dagger$  (The human's perception) before and after applying the washout filter. The subscription  $a$  and  $s$  denote actual motion and simulator, respectively. The final time in Eq. (11) is defined by  $t_f$ .

An overview of what is being done in this paper is shown in Figure 6. In this flowchart, the three spaces of roll, pitch, and heave are examined by the washout filter.

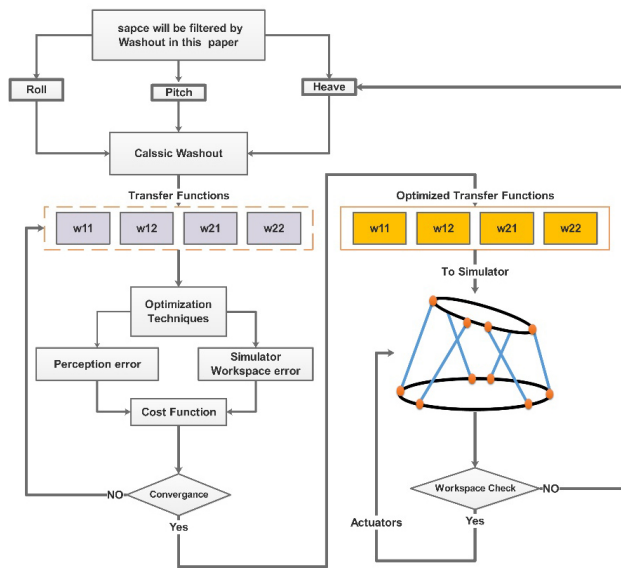


Figure 6. Proposed washout procedure in this paper

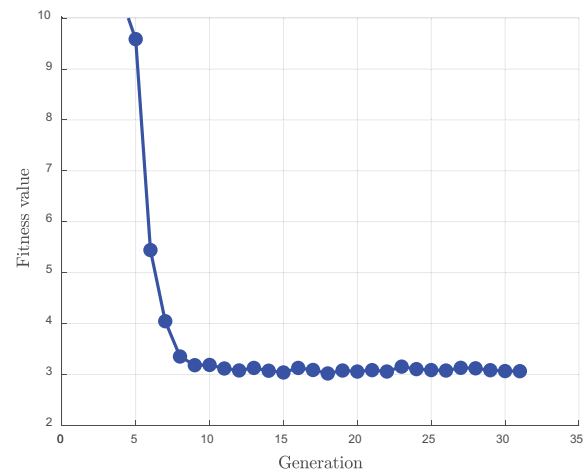


Figure 7. The generation of genetic algorithm for converging

Using the basics of the classical filter and the placement of transfer functions (Eq. (10)), the body of this filter is prepared, then a practical cost function (Eq. (11)) is considered to reduce perception error and exclude the flight simulator from its physical constraint. Next, using optimization algorithms, the coefficients of classical filter functions will be obtained.

### 4. Results and discussion

#### 4.1. Result of optimization

Using these transfer functions and reference inputs, which have been gained from experimental data, the pitch angle in a given robot compared with the sensation error of humans has been minimized. Table 1 displays the human vestibular model parameters for Otolith and semicircular systems (Chen & Fu, 2011).

Table 1. Parameters for otolith and semicircular model

Parameter	Surge	Sway	Heave	Roll	Pitch	Yaw
$\tau_l$	5.33	5.33	5.33	6.1	5.3	10.2
$\tau_s$	0.66	0.66	0.66	0.1	0.1	0.1
$\tau_a$	13.2	13.2	13.2	30	30	30
$k$	0.4	0.4	0.4			–
$d_{th}$	0.17	0.17	0.28	3.0	3.6	2.6

Three maneuvers (roll, pitch, and heave) are considered. The simulation time is about 25 sec for every generation of genetic algorithms. After ten generations, GA is converged, as shown in Figure 7.

The achieved denominator and numerator parameters  $W_{ij}$  are shown in Table 2, respectively. The optimized parameters are shown in Table 2 and then used in the rest of the simulation. These 78 parameters (72 coefficients of the numerator, six coefficients of the denominator) are used

for three different maneuvers (roll, pitch, and heave). The object function for each maneuver is defined as (Eq. (11)) which the main objects are minimizing the perception of the motion and being in the flight simulator workspace.

The details of simulated maneuvers are shown in Figure 8, where the angle/position and rate and acceleration are depicted separately. As the heave position (Figure 8g) shows, the position is in the flight simulator workspace interval, which satisfies the objective function’s first part. The fixed dashed red lines show the constraint of the flight simulator.

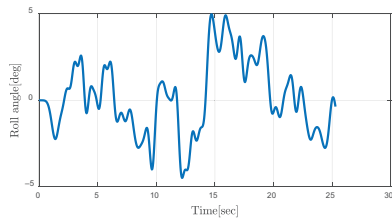
The perception rate of roll, pitch, and heave maneuvers is also shown in Figure 9. The perception function is compared for a maneuver before and after filtering by washout. As Figure 9 show, there is a time difference between signals. To compare accurately, the difference between the two signals plotted separately. Moreover, the average of the achieved error is depicted. This part of the simulation is satisfying the second part of the objective function.

To examine the correlation of motion perception for our study, the coefficient of determination ( $R^2$ ) is employed. The results show in Figure 10 that this value is 80.6%, 87%, and 93.7% for roll, pitch, and heave motions, respectively, which shows a reliable correlation for the perception system. It means that although the washout algorithm could decrease the actual acceleration in the flight simulator workspace, the perception system could sense the same earlier acceleration.

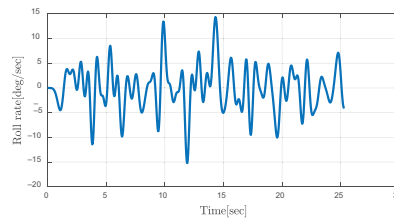
To compare the existing algorithm (i.e., GA) with another method (PSA: Pattern Search Algorithm) (Gharib et al., 2011), a particular mode of using a washout filter is used to improve the understanding of roll motion using the objective function (Eq. (12)). In this case, both algorithms’ convergence rates are compared with each other, which is shown in Figures 11–12. Figures 11–12 show that the rate of convergence has been done in generations and iterations. Also, the error of roll rate perception (RRP)

Table 2. The values of numerators and denominator for  $W_{ij}$  transfer functions (Numerators and denominator) in roll, pitch, and heave maneuver

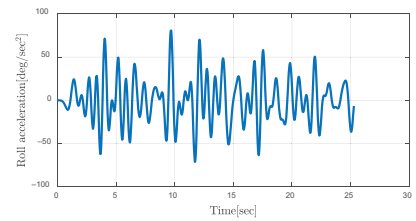
Maneuverer	TF No.	Numerator's Coefficients						
		$a_5$	$a_4$	$a_3$	$a_2$	$a_1$	$a_0$	
Roll	$W_{11}$	0.9872	0.8983	0.3011	0.1190	0.0035	0.0013	
	$W_{12}$	0.0013	0.2331	0.0976	0.3619	1.1184	1.2837	
	$W_{21}$	1.0336	1.0170	1.3860	0.2561	0.0357	0.2326	
	$W_{22}$	0.0887	1.4112	0.3612	0.0276	0.8910	0.2222	
Pitch	$W_{11}$	0.9999	0.8482	0.3884	0.2521	0.0006	0.0088	
	$W_{12}$	0.0022	0.0206	0.0000	0.6918	0.9220	0.1464	
	$W_{21}$	0.9897	0.1299	0.7442	0.4671	0.5046	0.9213	
	$W_{22}$	0.1786	0.3786	0.2153	0.9794	0.9508	0.0977	
Heave	$W_{11}$	1.1257	0.3900	0.2958	0.1567	0.6629	0.1035	
	$W_{12}$	0.1357	1.3235	1.2809	0.5590	0.3863	0.3337	
	$W_{21}$	0.5686	0.0809	0.2138	0.7118	0.9460	0.6268	
	$W_{22}$	1.1750	1.2600	0.4869	0.4561	1.4537	0.9496	
			Denominator's Coefficients					
	$W_{ij}$	$b_5$	$b_4$	$b_3$	$b_2$	$b_1$	$b_0$	
$W_{ij}, i, j = 1 : 2$	1.0000	0.8410	0.3585	0.0861	0.0098	0.0004		



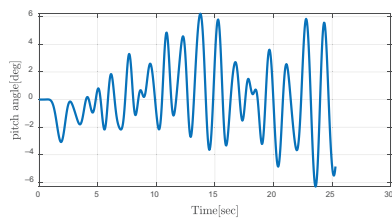
a) Roll angle



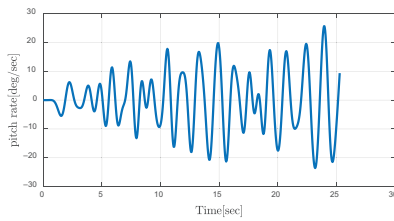
b) Roll rate



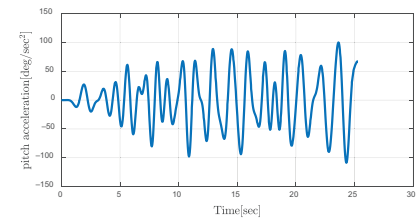
c) Roll acceleration



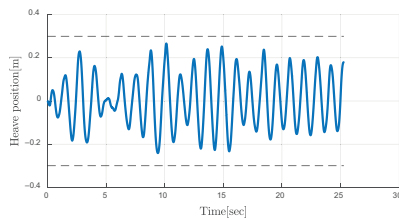
d) Pitch angle



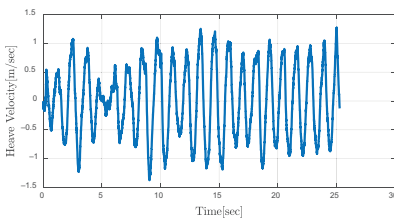
e) Pitch rate



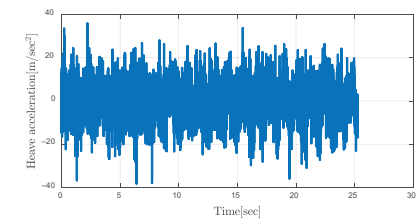
f) Pitch acceleration



g) Heave position

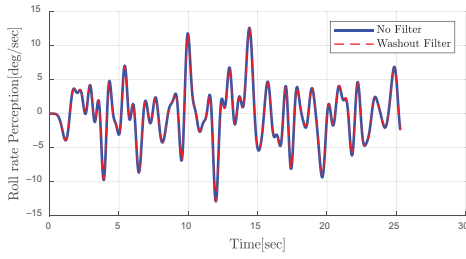


h) Heave velocity

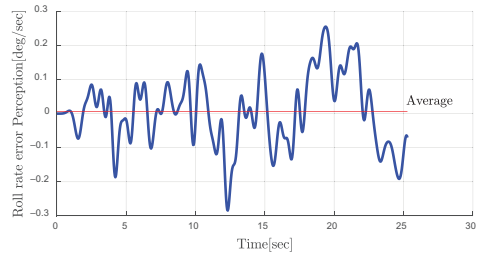


i) Heave acceleration

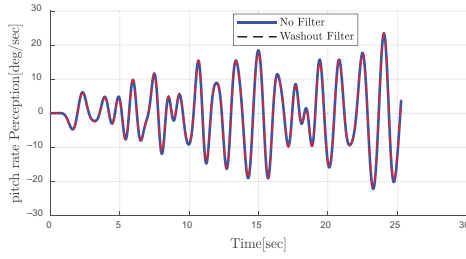
Figure 8. Maneuver detail filtered by proposed washout algorithm for (roll, pitch, and heave)



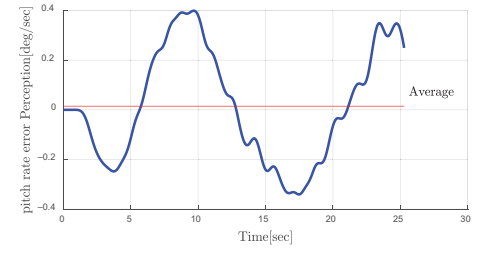
a) Roll rate perception



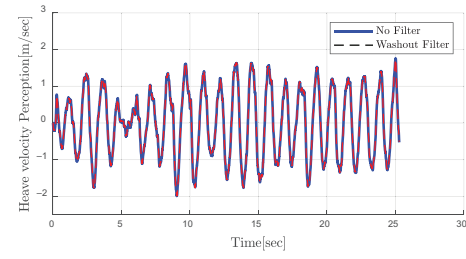
b) Roll rate perception error



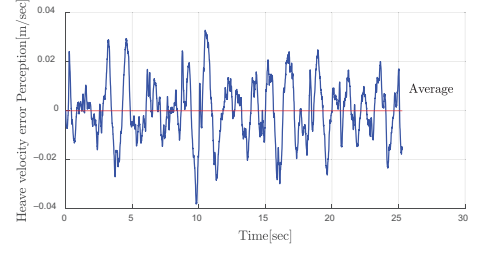
c) Pitch rate perception



d) Pitch rate perception error

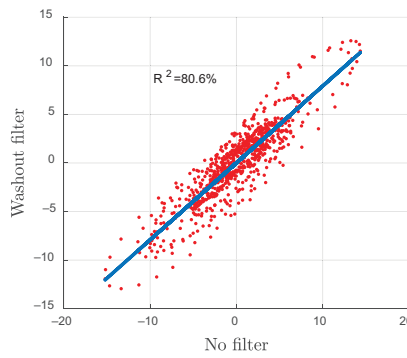


e) Heave velocity perception

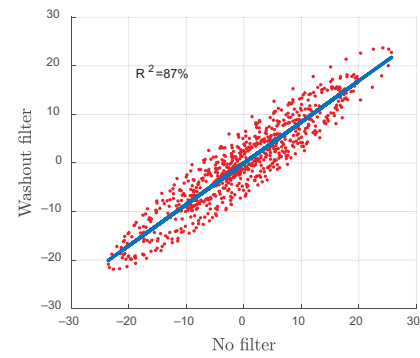


f) Heave velocity perception error

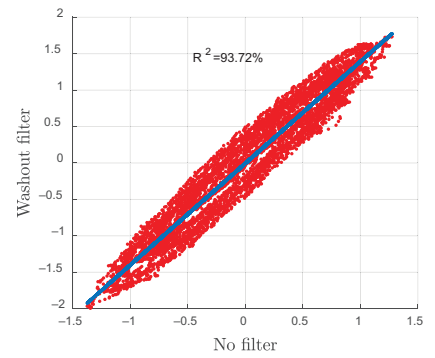
Figure 9. Maneuver rate perception and its error with no filter and with washout filter for (roll, pitch, and heave)



a) Roll



b) Pitch



c) Heave

Figure 10. The correlation of motion perception before and after washout installation

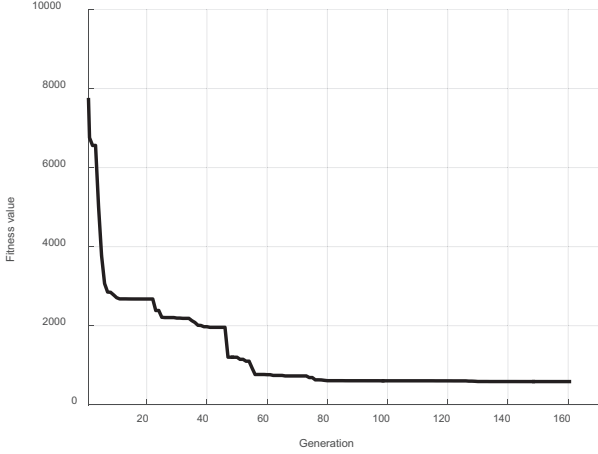


Figure 11. Converging of Genetic algorithm for Eq. (12)

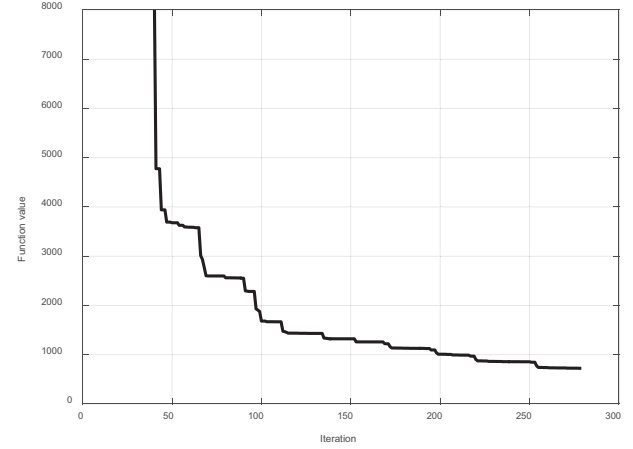


Figure 12. Converging of Pattern Search algorithm for Eq. (12)

diagram obtained is compared with both algorithms simultaneously, shown in Figure 12. Figure 12 shows that PSA provides a similar response to GA.

$$CF = \int_0^{t_f} t(\text{Error}_{\text{Roll}}) dt. \quad (12)$$

#### 4.2. Result of sensitivity

To compare other evolutionary methods with a different method and investigate the changes in the coefficients of the transfer functions in the performance of the washout filter, we study the denominator coefficients of the transfer functions. In this way, we change each of the five coefficients  $b_4: b_0$  according to Table 2 and then extracted them in an interval as Table 3. The coefficient  $b_5$  is assumed to be equal to one. The overall experiments ( $5^5 = 3125$ ) are time-consuming, so the Taguchi method is employed to decrease them. According to the orthogonal table  $L_{25}$  proposed by the Taguchi method, the number of experiments is reduced to 25, as shown in Table 4. Each of the experiments followed by an error that is consistent with Eq. (12).

In the Taguchi method, a statistic is introduced as the signal-to-noise ratio that can study the final result in three states: minimum, maximum, and normal (Goharimanesh & Akbari, 2015; Goharimanesh et al., 2014; Javadpour et al., 2020; Samavi et al., 2018). Since this article wants to minimize the error, the smaller better criterion introduced in Eq. (13) is chosen, where CF is the cost function defined in Eq. (12).

Table 3. factors and their levels

Factors-Levels	Symbol	1	2	3	4	5
$b_4$	A	0.7	0.75	0.8	0.85	0.9
$b_3$	B	0.2	0.25	0.3	0.35	0.4
$b_2$	C	0.07	0.075	0.08	0.085	0.09
$b_1$	D	0.008	0.0085	0.009	0.0095	0.01
$b_0$	E	0.0003	0.00035	0.0004	0.00045	0.0005

$$SNR = -10 \log(CF^2). \quad (13)$$

The result of this equation is shown in Figure 13. The maximum level for each factor indicates the optimal value of that factor. Also, the horizontal shape of a factor means

Table 4. design of experiments by Taguchi method

No.	$b_4$	$b_3$	$b_2$	$b_1$	$b_0$	CF
1	0.7	0.2	0.07	0.008	0.0003	2293.569
2	0.7	0.25	0.075	0.0085	0.00035	1987.723
3	0.7	0.3	0.08	0.009	0.0004	1891.028
4	0.7	0.35	0.085	0.0095	0.00045	1860.66
5	0.7	0.4	0.09	0.01	0.0005	1851.627
6	0.75	0.2	0.075	0.009	0.00045	2067.014
7	0.75	0.25	0.08	0.0095	0.0005	1531.248
8	0.75	0.3	0.085	0.01	0.0003	1343.46
9	0.75	0.35	0.09	0.008	0.00035	1298.566
10	0.75	0.4	0.07	0.0085	0.0004	1341.751
11	0.8	0.2	0.08	0.01	0.00035	1963.166
12	0.8	0.25	0.085	0.008	0.0004	1060.35
13	0.8	0.3	0.09	0.0085	0.00045	849.9414
14	0.8	0.35	0.07	0.009	0.0005	1013.976
15	0.8	0.4	0.075	0.0095	0.0003	829.2576
16	0.85	0.2	0.085	0.0085	0.0005	1552.481
17	0.85	0.25	0.09	0.009	0.0003	1010.764
18	0.85	0.3	0.07	0.0095	0.00035	893.4138
19	0.85	0.35	0.075	0.01	0.0004	726.7158
20	0.85	0.4	0.08	0.008	0.00045	729.922
21	0.9	0.2	0.09	0.0095	0.0004	1696.595
22	0.9	0.25	0.07	0.01	0.00045	1472.211
23	0.9	0.3	0.075	0.008	0.0005	1160.259
24	0.9	0.35	0.08	0.0085	0.0003	962.136
25	0.9	0.4	0.085	0.009	0.00035	927.2316

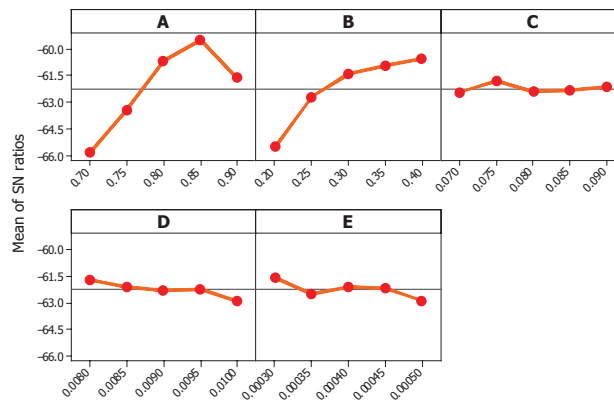


Figure 13. Signal to Noise Ratios for five factors versus their levels

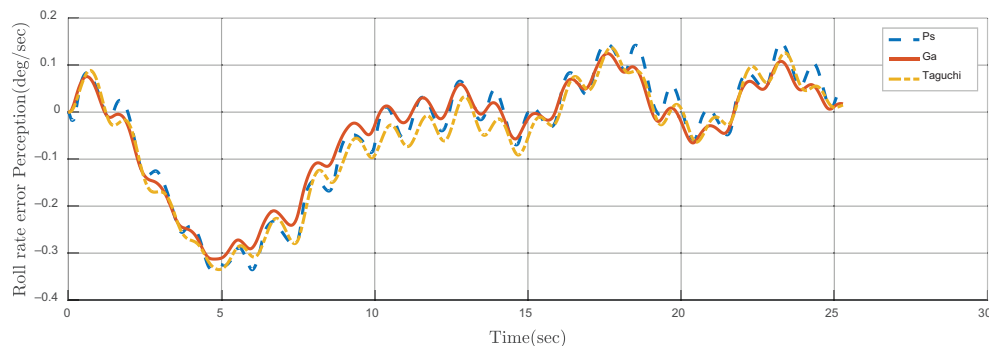


Figure 14. The error of roll rate perception (PRR) for GA, PS, and Taguchi

that it is insignificant, while its verticality means that it is important. As it shows, the first two coefficients  $b_4$  and  $b_3$ , are the most significant coefficients of the transfer functions, respectively. This result can later be used to improve the performance of an optimization algorithm for in-depth investigation.

The optimal states of the obtained coefficients and the coefficients obtained from the two evolutionary optimization algorithms are shown in Figure 14. As it is clear, the genetic algorithm could have performed better than the other two algorithms.

## Conclusions

One of the most famous challenges in the motion cueing algorithm is allocating the actuator's values to control human perception and make an actual motion in a real workspace for the flight simulators. In this paper, an evolutionary optimal washout filter (EOWF) decreases the human perception error and prepares an actual motion in the flight simulators workspace. The proposed filter inspires the optimal theory based on a genetic algorithm (Evolutionary algorithm) with defining an objective function that describes two criteria (minimizing the flight simulator's workspace and minimizing the human perception error). Three different maneuvers (roll, pitch, and heave) are considered, and the EOWF is implemented for each one separately, where GA is converged in fewer than 30

generations for allocating the proper values of the EOWF's parameters. The results show the actual motion proceeds in the real workspace (fewer than 30 cm in heave position), and the perception error decreased dramatically in which correlations of human perception before and after applying the proposed washout filter are upper than 80% for all of the proposed maneuvers (i.e., the human perception is not changed intensely when the washout filter is applied). The proposed washout filter (EOWF) decreases the actual acceleration in the flight simulator workspace and the perception system's error simultaneously.

## References

- Affan, M., Ahmed, S. U., Manek, A. I. y., & Uddin, R. (2019, 11–12 December). Design and implementation of the washout filter for the Stewart-Gough Motion Platform. In *2019 International Conference on Computational Intelligence and Knowledge Economy (ICCIKE)* (pp. 415–419). Dubai, UAE. <https://doi.org/10.1109/ICCIKE47802.2019.9004317>
- Arioui, H., Nehaoua, L., & Amouri, A. (2005). Classic and adaptive washout comparison for a low cost driving simulator. In *Proceedings of the 2005 IEEE International Symposium on, Mediterrean Conference on Control and Automation* (pp. 586–591). IEEE. <https://doi.org/10.1109/2005.1467080>
- Asadi, H., Lim, C. P., Mohamed, S., Nahavandi, D., & Nahavandi, S. (2019). Increasing motion fidelity in driving simulators using a fuzzy-based washout filter. *IEEE Transactions on Intelligent Vehicles*, 4(2), 298–308. <https://doi.org/10.1109/TIV.2019.2904388>



- Asadi, H., Mohamed, S., Lim, C. P., & Nahavandi, S. (2016). Robust optimal motion cueing algorithm based on the linear quadratic regulator method and a genetic algorithm. *IEEE Transactions on Systems, Man, and Cybernetics: Systems, PP(99)*, 1–17. <https://doi.org/10.1109/TSMC.2016.2523906>
- Chen, S. H., & Fu, L.-C. (2011, August). An optimal washout filter design with fuzzy compensation for a motion platform. In *18th IFAC World Congress, IFAC Proceedings Volumes*, 44(1), 8433–8438. <https://doi.org/10.3182/20110828-6-IT-1002.03176>
- Chen, S. H., & Fu, L. C. (2010). An optimal washout filter design for a motion platform with senseless and angular scaling maneuvers. *IFAC Proceedings Volumes*, 44(1), 8433–8438. <https://doi.org/10.1109/ACC.2010.5530820>
- Gharib, M. R., Kamelian, S., Seyyed Mousavi, S. A., & Dabzadeh, I. (2011). Modelling and multivariable robust controller for a power plant. *International Journal of Advanced Mechatronic Systems*, 3(2), 119–128. <https://doi.org/10.1504/IJAMECHS.2011.040683>
- Gharib, M. R. (2020). Comparison of robust optimal QFT controller with TFC and MFC controller in a multi-input multi-output system. *Reports in Mechanical Engineering*, 1(1), 151–161. <https://doi.org/10.31181/rme200101151g>
- Gharib, M. R., Koochi, A., & Ghorbani, M. (2021). Path tracking control of electromechanical micro-positioner by considering control effort of the system. *Proceedings of the Institution of Mechanical Engineers, Part I: Journal of Systems and Control Engineering*, 235(6), 984–991. <https://doi.org/10.1177/0959651820953275>
- Goharimanesh, M., & Akbari, A. (2015). Optimum parameters of nonlinear integrator using design of experiments based on Taguchi method. *Journal of Computational Applied Mechanics*, 46(2), 233–241.
- Goharimanesh, M., Akbari, A., & Akbarzadeh Tootoonchi, A. (2014). More efficiency in fuel consumption using gearbox optimization based on Taguchi method. *Journal of Industrial Engineering International*, 10(2), 61. <https://doi.org/10.1007/s40092-014-0061-y>
- Grant, P. R., & Reid, L. D. (1997). Motion washout filter tuning: Rules and requirements. *Journal of Aircraft*, 34(2), 145–151. <https://doi.org/10.2514/2.2158>
- Huang, C., & Fu, L. (2006, 8–11 October 2006). Human Vestibular Based (HVB) Senseless maneuver optimal washout filter design for VR-based motion simulator. In *2006 IEEE International Conference on Systems, Man and Cybernetics* (pp. 4451–4458). Taipei, Taiwan. <https://doi.org/10.1109/ICSMC.2006.384835>
- Javadpour, S. M., Abbasi Jannat Abadi, E., Akbari, O. A., & Goharimanesh, M. (2020). Optimization of geometry and nano-fluid properties on microchannel performance using Taguchi method and genetic algorithm. *International Communications in Heat and Mass Transfer*, 119, 104952. <https://doi.org/10.1016/j.icheatmasstransfer.2020.104952>
- Kim, K. D., Kim, M. S., Moon, Y. G., & Lee, M. C. (2006, October 18, 2006–October 21). Application of vehicle driving simulator using new washout algorithm and robust control. In *2006 SICE-ICASE International Joint Conference* (pp. 2121–2126). Busan, Korea, Republic of. <https://doi.org/10.1109/SICE.2006.315563>
- Kong, X.-T., Zhu, Y.-C., Di, Y.-Q., & Cui, H.-H. (2016). Methods to determine optimal washout position for single and multi-occupant motion simulator. *Cybernetics and Information Technologies*, 16(1), 173–187. <https://doi.org/10.1515/cait-2016-0014>
- Liao, C.-S., Huang, C.-F., & Chieng, W.-H. (2004). A novel washout filter design for a six degree-of-freedom motion simulator. *JSME International Journal Series C Mechanical Systems, Machine Elements and Manufacturing*, 47(2), 626–636. <https://doi.org/10.1299/jsmec.47.626>
- Liu, Z., Guo, Q., Jin, Z., & Yu, G. (2020). Research on a washout algorithm for 2-DOF motion platforms. In J. Y. C. Chen & G. Fragomeni (Eds). *Virtual, augmented and mixed reality. Design and Interaction. HCII 2020. Lecture Notes in Computer Science*, Vol. 12190. Springer. [https://doi.org/10.1007/978-3-030-49695-1\\_8](https://doi.org/10.1007/978-3-030-49695-1_8)
- Moavenian, M., Gharib, M. R., Daneshvar, A., & Alimardani, S. (2011, August). Control of human hand considering uncertainties. In *The 2011 International Conference on Advanced Mechatronic Systems* (pp. 17–22). IEEE.
- Mohammadi, A., Asadi, H., Mohamed, S., Nelson, K., & Nahavandi, S. (2018a). Multiobjective and interactive genetic algorithms for weight tuning of a model predictive control-based motion cueing algorithm. *IEEE Transactions on Cybernetics*, 49(9), 3471–3481. <https://doi.org/10.1109/TCYB.2018.2845661>
- Mohammadi, A., Asadi, H., Mohamed, S., Nelson, K., & Nahavandi, S. (2018b). Optimizing model predictive control horizons using genetic algorithm for motion cueing algorithm. *Expert Systems with Applications*, 92, 73–81. <https://doi.org/10.1016/j.eswa.2017.09.004>
- Nahon, M. A., Reid, L. D., & Kirdeikis, J. (1992). Adaptive simulator motion software with supervisory control. *Journal of Guidance, Control, and Dynamics*, 15(2), 376–383. <https://doi.org/10.2514/3.20846>
- Nehaoua, L., Mohellebi, H., Amouri, A., Arioui, H., Espie, S., & Kheddar, A. (2008). Design and control of a small-clearance driving simulator. *IEEE Transactions on Vehicular Technology*, 57(2), 736–746. <https://doi.org/10.1109/TVT.2007.905336>
- Parrish, R. V., Dieudonne, J. E., Bowles, R. L., & Martin Jr, D. J. (1975). Coordinated adaptive washout for motion simulators. *Journal of Aircraft*, 12(1), 44–50. <https://doi.org/10.2514/3.59800>
- Qazani, M. R. C., Asadi, H., Bellmann, T., Mohamed, S., Lim, C. P., & Nahavandi, S. (2020). Adaptive washout filter based on fuzzy logic for a motion simulation platform with consideration of joints limitations. In *IEEE Transactions on Vehicular Technology*, 69(11), 12547–12558. <https://doi.org/10.1109/TVT.2020.3023478>
- Salehi Kolahi, M. R., Gharib, M. R., & Heydari, A. (2021). Design of a non-singular fast terminal sliding mode control for second-order nonlinear systems with compound disturbance. *Proceedings of the Institution of Mechanical Engineers, Part C: Journal of Mechanical Engineering Science*, 235(24), 7343–7352. <https://doi.org/10.1177/09544062211032990>
- Salehi Kolahi, M. R., Gharib, M. R., & Koochi, A. (2021). Design of a robust control scheme for path tracking and beyond pull-in stabilization of micro/nano-positioners in the presence of Casimir force and external disturbances. *Archive of Applied Mechanics*, 91(10), 4191–4204. <https://doi.org/10.1007/s00419-021-02002-3>
- Samavi, J., Goharimanesh, M., Akbari, A., & Dezyani, E. (2018). Optimisation of drilling parameters on St37 based on Taguchi method. *Journal of the Brazilian Society of Mechanical Sciences and Engineering*, 40(8), 370. <https://doi.org/10.1007/s40430-018-1245-y>
- Sivan, R., Ish-Shalom, J., & Huang, J. (1982). An optimal control approach to the design of moving flight simulators. *IEEE Transactions on Systems, Man, and Cybernetics*, 12(6), 818–827. <https://doi.org/10.1109/TSMC.1982.4308915>

- Song, C.-C., Liaw, D.-C., & Chung, W.-C. (2002, October 28–October 31). Washout-filter based bifurcation control of longitudinal flight dynamics. In *2002 IEEE Region 10 Conference on Computers, Communications, Control and Power* (pp. 1646–1649). Beijing, China. <https://doi.org/10.1109/TENCON.2002.1182648>
- Telban, R., Cardullo, F., & Houck, J. A. (2002, August 5). Non-linear, human-centered approach to motion cueing with a neurocomputing solver. In *AIAA Modeling and Simulation Technologies Conference and Exhibit* (pp. 1–10). Monterey, CA, USA. <https://doi.org/10.2514/6.2002-4692>
- Wang, S. C., & Fu, L. C. (2004, October 10, 2004–October 13). Predictive washout filter design for VR-based motion simulator. In *IEEE International Conference on Systems, Man and Cybernetics, SMC 2004*, 6291–6295. The Hague, Netherlands. <https://doi.org/10.1109/ICSMC.2004.1401387>
- Wang, X. L., Li, L., & Zhang, W. (2008). Parameters optimization of the classical washout algorithm in locomotive driving simulator. *Zhongguo Tiedao Kexue/China Railway Science*, 29(5), 102–107.
- Wang, X. L., Li, L., & Zhang, W. H. (2010). Research on fuzzy adaptive washout algorithm of train driving simulator. *Tiedao Xuebao/Journal of the China Railway Society*, 32(2), 31–36.
- Yang, Y., Huang, Q.-T., & Han, J.-W. (2010). Adaptive washout algorithm based on the parallel mechanism motion range. *Xi Tong Gong Cheng Yu Dian Zi Ji Shu/Systems Engineering and Electronics*, 32(12), 2716–2720.